Piotr JÓŹWIAK*, Krzysztof SICZEK*

RESEARCH ON FRICTION RESISTANCE IN THE CONCENTRATED CONTACT STEEL –ON-MAGNESIUM ALLOY

BADANIE OPORU RUCHU W SKONCENTROWANYM STYKU STALI PO STOPIE MAGNEZU

Key words:

steel, magnesium alloy, friction coefficient, concentrated contact

Słowa kluczowe:

stal, stop magnezu, współczynnik tarcia, styk skoncentrowany

Summary

Magnesium alloys used in the automotive industry because of low density and the good strength sometimes mate with steel elements. The aim of the research has been to investigate friction resistance in contact steel-on-AM60 (Mg6Al0.15Mn) alloy and to find a way to decrease such resistance. Difficult mating conditions of such elements can be improved by surface treatment, i.e. plasma or laser modification. Values of the friction coefficient have been decreased with an almost linear mean stress increase. Using a tribotester for spinning friction, presented in the article, values of friction coefficient

* Politechnika Łódzka, Katedra Pojazdów i Podstaw Budowy Maszyn, ul. Żeromskiego 116, 90-924 Łódź, tel. 426312250, e-mail: ks670907@p.lodz.pl, e-mail: piotr.jóźwiak@wp.pl.

in contact LH15-on-AM60 (Mg6Al0.15Mn) alloy have been 2.5 times higher than respective values obtained in the LH15-on-C45 contact zone and can be twice as high when compared to values obtained in the case of pin-on-disc tester. This can be because of a higher value of mean surface pressure and mean sliding speed in the case of a tester for spinning friction.

INTRODUCTION

In the automotive industry there is currently a widespread tendency to reduce the weight of all vehicle components. One method is based on the use of lightweight materials in place of steel. Here aluminium alloys are of the largest share. Magnesium alloys that are of lower density (up to 25% of aluminium alloys) have not been widely applied **[L. 1]**. Automotive elements made of magnesium alloys can be forged or cast under pressure. So far, magnesium alloy has been used primarily for the manufacture of wheels. The use of magnesium alloys for the manufacture of the body parts has been difficult due to the structurally limited cold deformability **[L. 2]**. Underdeveloped technology of magnesium is one of the barriers that limits its use in production. This is despite the high prevalence of magnesium, easy and safe recycling and despite the well-known cases of execution of magnesium sheet metal for aerospace components that meet the highest requirements for durability and surface quality.

Magnesium is suitable for structural components and has a low strength to weight ratio and stiffness, particularly in bending and buckling loads **[L. 2]**.

Magnesium sheets have many advantages in relation to cast and forged elements. This is due to its homogeneous and fine structure with a small number of defects. The result is a higher strength, better ductility from the treatment, the greater load bearing during operation and greater energy absorption by the occurrence of deformation under load **[L. 2]**. The latter can be used in the design of the crumple zone of an automotive body. Currently, there are methods of manufacturing thin-walled, high-quality surfaces and reproducible mechanical properties for elements made of magnesium alloys **[L. 1–4]**.

Compared to materials with plastic properties, magnesium alloys have better temperature properties and can operate at much higher temperatures, and the thermal expansion is lower and is easier to use as a secondary raw material **[L. 1]**.

Magnesium alloys reduce vibration well and are easily machined. The high thermal conductivity make them difficult for ignition and burning. Magnesium alloy's disadvantage is its susceptibility to corrosion and the need for careful corrosion protection **[L. 2]**.

Magnesium alloys have poor formability and limited ductility at room temperature, which ascribed to their hexagonal close-packed (HCP) crystal structure **[L. 1]**.

Nowadays, AZ31 (MgAl3Zn1) **[L. 2, 3]**, and also AZ61 (MgAl6Zn1) **[L. 2, 3]**, ZK60 (MgZn6Zr1) **[L. 3]**, AM60 (MgAl6Mn0.15) **[L. 4]**, MA2 (MgAl4Zn1) **[L. 5, 6]**, AZ91 (MgAl9Zn1) **[L.** 6], and WE43 (Mg-4Y-2.4Nd-3.3RE (heavy rare earth)-0.55Zr) **[L. 3]** are commonly used as magnesium wrought alloys.

There some cases when the friction contact takes place between one part made of steel and the other made of magnesium alloy. One group includes steel fasteners against bumpers and steel nuts against the rack of steering wheels, when a high value of friction coefficient is beneficial. In such contacts, fretting phenomena can take place. The second group, when value of friction coefficient should be low, includes the following:

– Steel balls against a cage made of magnesium alloy (in high speed roller bearings lubricated by oil or grease), and
– Steel balls against ball slide made of magnesium alloy (Such slides are low loaded and can operate in absence of oil, and they can be used in some cases of sliding parts like ramps, doors, shelves, and chairs especially in recreational and repair vehicles.),

The aim of the researches presented in this article is to investigate the friction resistance in contact steel–on-magnesium alloy AM60 (MgAl6Mn0.15) and to find a way to decrease such resistance.

3. METHODS IMPROVING THE WEAR RESISTANCE OF WROUGHT MAGNESIUM ALLOYS

The behaviour of magnesium alloys for forming in friction contact is not sufficiently investigated. The results from **[L. 7]** can be cited, which were obtained during tests for a step in the modification of the surface layer for the AZ31 (MgAl3Zn1) alloy as a result of the friction process in the contact with chlorine-sulfonated polyethylene, plasticized polyvinyl chloride, ebonite, sulphur vulcanizate of styrene-butadiene rubber, and polysulphide rubber and polysulfone. There has been a modification of the surface layer of the AZ31 (MgAl3Zn1) alloy, occurring as a result of the transfer of S, Cl- ions, and fragments of polymer chains containing such ions. Oxides and unidentified compounds of carbon and hydrogen have also been observed. The influence of tribochemical modification on the tribological characteristics of joints metal--on-polymer has been shown.

Some of technological difficulties arise in the implementation of sliding contacts for elements made of magnesium alloys with the elements made of steel. Such difficulties can be overcome by the use of surface treatments for magnesium alloys.

Some new surface treatment technologies of magnesium alloys have been reported, such as plasma electrolytic oxidation **[L. 8]**, microarc oxidation **[L. 9]**, electronic beam, and laser modification **[L. 10–12]**, ion beam assisted evaporation deposition **[L. 13]**, and chemical plating **[L. 14]**. Among them, the normal

plasma beam has many advantages: similar power density to laser beam, simple plasma generator, favourable environment, non-limitation to specimen size, and the designed structure of plasma generator according to part shapes and processing conditions **[L. 15]**. A plasma beam **[L. 16]** can be used as an alternative for a laser beam **[L. 16–17]**. The plasma melting process can be used to improve the wear resistance of AM60 (MgAl6Mn0.15) alloy. This process can be attributed to the decrease in the amount of porosity, grain size, and the strengthening of the produce solid solution. After plasma melting, grain size is decreased less than 1pm due to the quick cooling rate and β-Mgi7Ali2 is well distributed in the melted layer. The plasma melting is a simple and cheap surface modification method for AM60 (MgAl6Mn0.15) **[L. 16]**.

MECHANICAL PROPERTIES OF AM60 (MgAl6Mn0.15) ALLOY

The mechanical properties of AM60 (MgAl6Mn0.15) alloy have investigated at different strain rates and are described in **[L. 18]**. The impact energy of this alloy increased nonlinearly with temperature increase.

The tensile test have indicated that the mechanical properties have not been sensitive to the strain rates applied ($3.3x10^{-4}$~0.1), and the plastic deformation was dominated by twining mediated slip. The impact energy is not very sensitive to the environmental temperature **[L. 18]**. It is equal to 5.35 J at room temperature. The plane strain fracture toughness and fatigue limit were evaluated and the average values were 7.6 MPa.m1/2 and 25 MPa, respectively **[L. 18]**.

Friction force in the contact steel-on-AM60 (MgAl6Mn0.15) alloy have been investigated and the results have been presented in **[L. 19]**. The morphology of AM60 (MgAl6Mn0.15) alloy has been composed of α-Mg matrix and irregular β —precipitation along grain boundaries (Mg17Al12). For AM60 (MgAl6Mn0.15) alloy, the reduction of aluminium has been accompanied by greatly decreasing of β-phase **[L. 19]**.

Wear tests have been conducted using a pin-on-disc type apparatus. In these tests, a sample made of AM60 (MgAl6Mn0.15) alloy was mated with the rotating disc made of steel 5CrNiMo with a hardness of HRC = 55. The experiments were carried out under dry friction conditions in an environment of 25ºC. The speed of the disc employed was 0.628 m·s-1. The AM60 (MgAl6Mn0.15) sample had dimensions of Ø6 mm x 12 mm, and the steel disc had dimensions of Ø70 mm x 10 mm. The range of loads was 20-1l0 N **[L. 19]**.

The surface of the wear test samples were polished to obtain surface roughness, Ra, up to 0.3 μm. The disc and specimen were cleaned with acetone to remove any possible traces of grease and other surface contaminants. Based on data from **[L. 19]**, the dependence of the friction coefficient on the calculated mean surface pressure was determined and presented in **Figure 1**. Rhombus mean of original data is from **[L. 19]**. This dependence is of a decreasing power

series shape, and it allows the rough estimation of values of the friction coefficient for the case of values of the mean surface pressure σ_{mean} higher than 500 MPa, which are closer to those obtained from the tester for spinning friction.

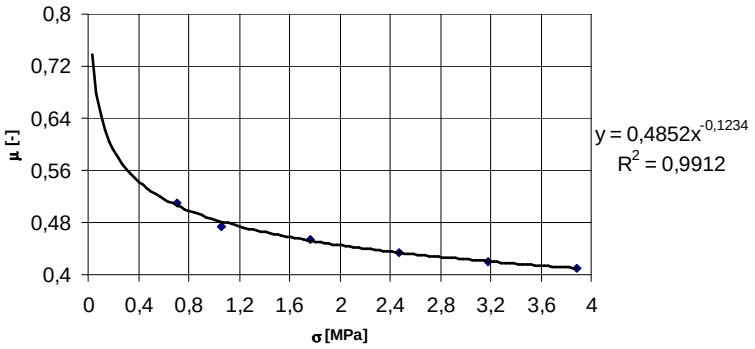

Fig. 1. Friction coefficient μ against mean surface pressure σ_{mean}
Rys. 1. Współczynnik tarcia μ w funkcji średniego nacisku powierzchniowego w styku.

The friction coefficient is reduced with an increase in the applied load and tends to be steady and gradual. Load affects wear behaviour by contact area and deformation. In the sliding process, the metal surface is in an elastic-plastic state and the real contacting area is not linearly related to the load, leading to the decrease of the friction coefficient with the increase of load.

DETERMINATION FOR VALUES OF THE FRICTION COEFFICIENT IN THE CONTACT BALL-ON-PLANE DISC

It has been assumed that the values of surface pressure in the contact zone ball-on-disc can be calculated from Hertz equations.

The friction moment M_t between the ball and rotating disc can be calculated from Equation (1) **[L. 20]**

$$M_t = 0.1875\pi\mu F r_0 \tag{1}$$

Where: F – the force loading contact zone ball-on-disc in the tester, μ – the friction coefficient.

The radius r_0 of contact zone between the ball and rotating disc has been calculated from Equation (2) **[L. 20]**

$$r_0 = \sqrt[3]{\frac{3}{4}\cdot F\left(\frac{1}{r_1}-\frac{1}{r_2}\right)^{-1}\left(\frac{1-\nu_1^2}{E_1}+\frac{1-\nu_2^2}{E_2}\right)} \tag{2}$$

Where: $r_1 = 0.004$ [m] – radius of the ball, $r_1 = \infty$ [m] – curvature radius of the plate, E_1 – the Young's modulus of the ball material, ν_1 – the Poisson's ratio of the ball material, E_2 – the Young's modulus of the disc material, ν_2 – the Poisson's ratio of the disc material

From Equations (1) and (2) the friction coefficient μ can be estimated.

EXPERIMENTAL RESEARCH

The research was carried out on the tribotester for measuring the contact resistance in a concentrated contact ball-on-disc in conditions of spinning friction. The scheme of the tribotester is presented in **Figure 2**. No additional oil lubrication was used in the contact zone, so technically dry friction conditions took place there. Such conditions take place during the operation of the ball slide. Estimated loading of the slide was up to 20 N. The estimated rotational speed of the balls was lower than 40 rpm.

During tests, the ball was fixed and the disc rotated with a speed of 36 rpm. The loading of the ball increased in stepwise manner from 7 – 16.9 N. The step of the load increase depended on the added weights (six pieces).

The threshold of the friction moment measured in the tester was 0.0005 Nm.

Tests were realized at room temperature and in a constant humidity of 40%.

The following two sets wer considered:

1. A ball made of LH15 steel and a disc made of AM60 (MgAl6Mn0.15) alloy,
2. A ball made of the LH15 steel and a disc made of C45 steel.

For each value of load F, the value of friction moment M_t between the ball and disc were measured during test. On the basis of these measurements, the progression of M_t(F) was obtained.

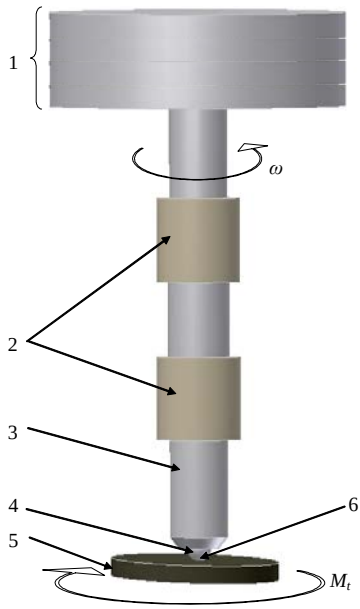

Fig. 2. The scheme of tribotester; 1 – weights, 2 – air bearing, 3 – stem, 4 – ball, 5 – disc, 6 – contact zone, M_t – the measured friction moment, ω – rotating speed

Rys. 2. Schemat tribotesteru; 1 – obciążniki, 2 – łożyska powietrzne, 3 – trzpień, 4 – kulka, 5 – płaska tarcza, 6 – strefa styku, M_t – mierzony moment tarcia, ω – prędkość obrotowa

The researched ball and the sample (disc) were weighted before and after the measurement of the friction moment M_t to estimate the amount of their mass wear. The resolution of the balance scale was equal 0.2 g.

RESULTS OF RESEARCH

The values of the friction coefficient were calculated based on mean value of the friction moment measured in the tribotester for six values of loading. The observed deviation of measured values from the mean values was 0.001 Nm. It corresponds to the deviation of calculated values of the friction coefficient 0.05.

The obtained dependences of friction coefficient on mean surface pressure are presented in **Figure 3** for contact LH15 steel-on-AM60 (MgAl6Mn0.15) alloy, and in Figure 4 for contact LH15-on-C45.

Values of the calculated friction coefficient decreased with the mean stress increase almost linearly. As observed in both cases of contact, the ball made of LH15 steel on a disc made of AM60 (MgAl6Mn0.15) alloy and between the ball made of LH15 steel on the disc made of C45 steel, the values of the friction coefficient in contact LH15-on-AM60 (MgAl6Mn0.15) were 2.5 times higher than respective values obtained in the LH15-on-C45 contact zone. Calculated from Equations (1)-(2), the values of friction coefficient in contact steel-on-AM60 (MgAl6Mn0.15) alloy, in the case of the tester for spinning friction, were nearly twice as high as the values obtained in the case of pin-on--disc tester. This can be because of the higher value of mean surface pressure and mean sliding speed in the case of the tester for spinning friction.

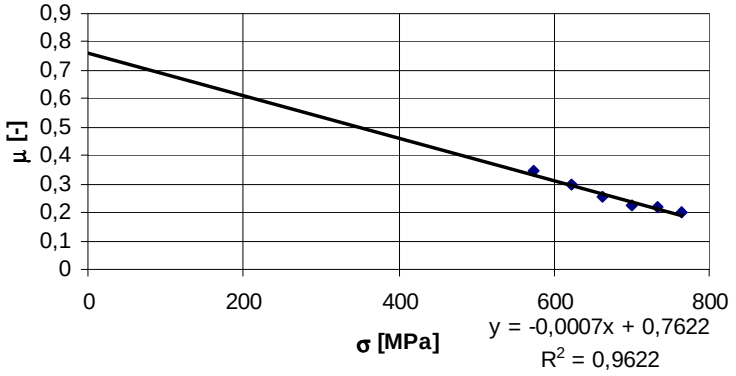

Fig. 3. The friction coefficient μ vs. mean surface pressure σ_{mean} in contact of LH15-AM60 (MgAl6Mn0.15)

Rys. 3. Współczynnik tarcia μ w funkcji średniego ciśnienia σ_{mean} w styku ŁH15-AM60 (MgAl6Mn0.15)

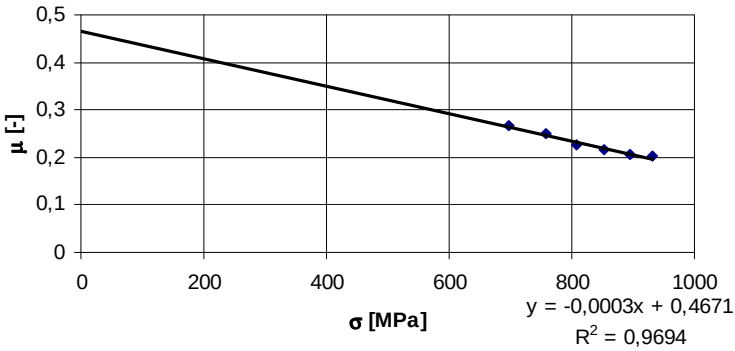

Fig. 4. The friction coefficient μ vs. mean surface pressure σ_{mean}, in contact of LH15-C45
Rys. 4. Współczynnik tarcia μ w funkcji średniego ciśnienia σ_{mean} w styku ŁH15-C45

The obtained amounts of mass wear for tested balls and samples were lower than the resolution of the balance scale. In addition, there were obvious signs of wear on the surfaces of tested balls and on the steel sample. More obvious signs of wear were obtained for the sample made of AM60 (MgAl6Mn0.15) alloy. **Figure 5** presents signs of wear on the sample made of AM60 (MgAl6Mn0.15) alloy after the measurement of the friction moment M_t

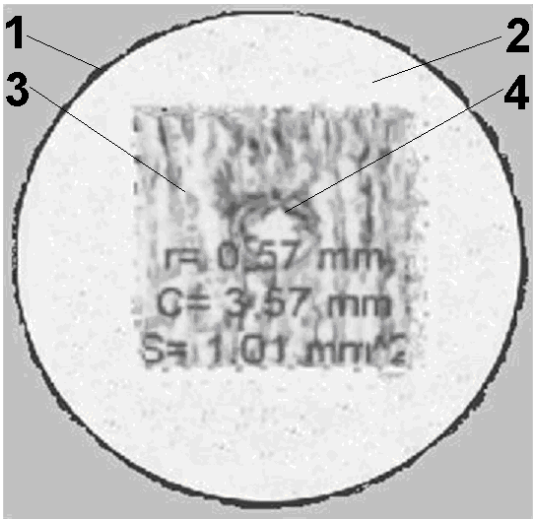

Fig. 5. The signs of wear on the sample made of AM60 (MgAl6Mn0.15) alloy after measurement of friction moment M_t in contact of LH15-AM60 (MgAl6Mn0.15); 1 – thin steel ring, 2 – cured epoxy resin, 3 – sample made of AM60 (MgAl6Mn0.15) alloy, 4 – signs of wear
Rys. 5. Ślady zużycia na płytce wykonanej ze stopu AM60 (MgAl6Mn0.15) po zmierzeniu momentu tarcia M_t w styku ŁH15-AM60 (MgAl6Mn0.15); 1 – cienki pierścień stalowy, 2 – utwardzona żywica epoksydowa, 3 – próbka ze stopu AM60 (MgAl6Mn0.15), 4 – ślady zużycia

in contact of LH15-AM60 (MgAl6Mn0.15) with force F loading of the contact zone equal to 16.9 N. Radius r of wear zone was 0.57 mm, and the depth c of wear zone was 3.67 mm. The area S of contact zone was 1.01 mm^2. The obtained amounts of wear were low because of the short time for the measurement of the friction moment M_t.

CONCLUSIONS

Values of the calculated friction coefficient decreased with the mean surface pressure increase almost linearly. This was observed in both cases of contact: ball made of LH15 steel-on-disc made of AM60 (MgAl6Mn0.15) alloy and ball made of LH15 steel-on-disc made of C45 steel. Values of friction coefficient in contact LH15-on-AM60 (MgAl6Mn0.15) were 2.5 times greater than respective values obtained in the LH15-on-C45 contact zone.

Estimated values of friction coefficient in contact steel-on-AM60 (MgAl6Mn0.15) alloy, in the case of tester for spinning friction, can be twice greater than values obtained in the case of pin-on-disc tester. This may be due to the greater value of the mean surface pressure and mean sliding speed in the case of tester for spinning friction.

High values of the friction coefficient in contact steel-on-AM60 (MgAl6Mn0.15) suggest the necessity of a surface treatment of AM60 (MgAl6Mn0.15) alloy to obtain higher wear resistance. The review of the literature suggests that it can be done by plasma or laser treatment.

REFERENCES

1. Li Jin, Dongliang Lin, Dali Mao, Xiaoqing Zeng, Wenjiang Ding, Mechanical properties and microstructure of AZ31 Mg alloy processed by two-step equal channel angular extrusion, Materials Letters, Vol. 59, Issue 18, August 2005, pp. 2267–2270.
2. Magnez w samochodach, Maszyny Technologie Materiały-Technika Zagraniczna, Nr 3/2005.
3. Hadasik E., Śliwa R.E., Nowoczesne technologie materiałowe stosowane w przemyśle lotniczym. ZB 7. Plastyczne kształtowanie stopów magnezu (kucie precyzyjne, tłoczenie, wyciskanie, walcowanie itp.), available at: http://pkaero.prz.edu.pl/sprawozdania/1-konferencja/zb71.pdf.
4. Ziółkiewicz S., Gąsiorkiewicz M., Wesołowska P., Szczepaniak S., Szyndler R., Wpływ obróbki KOBO na właściwości plastyczne stopu magnezu AM60, Obróbka Plastyczna Metali Vol. XXIII Nr 3 (2012). Inżynieria materiałowa w obróbce plastycznej, s. 149–158.
5. Gontarz A., Dziubińska A., Własności stopu magnezu MA2 (wg GOST) w warunkach kształtowania na gorąco, Rudy i Metale Nieżelazne 2010, R. 55, nr 6, s. 340–344.

6. Miura H., Yang X., Sakai T., Ultrafine Grain Evolution in Mg Alloys, AZ31, AZ61, AZ91 by Multidirectional Forging, Review of Advanced Materials Science, 33 (2013) pp. 92–96.
7. Siciński, M.; Bieliński, D.; Grams, J., Tribochemical modification of the surface layer of magnesium alloy AZ 31 counterface wearing against elastomer containing sulphur and chlorine, Tribologia: tarcie, zużycie, smarowanie, (2009), nr 2, pp. 225–232.
8. Cao F.H., Lin L.Y., Zhang Z., Zhang J.Q., Cao C.N., Environmental friendly plasma electrolytic oxidation of AM60 magnesium alloy and its corrosion resistance, Transactions of the Nonferrous Metals Socjety of China, Vol. 18 (2008), pp. 240–247.
9. Xue W.B., Jin Q., Zhu Q.Z., Hua M., Ma Y.Y., Anti-corrosion microarc oxidation coatings on SiC_P/AZ31 magnesium matrix composite, Journal of Alloys and Compounds Vol.482 (2009), p. 208–212.
10. Loveless J.D., Alemohammad H., Li J., Gertsman V., Emadi D., Toyserkani E., Esmaeili S., Laser-assisted maskless microdeposition of silver nano-particles on a magnesium substrate, Materials Letters, Vol. 63 (2009), pp. 1397–1400.
11. Bohne Y., Seeger D.M., Blawert C., Dietzel W., Mändl S. & Rauschenbach B. (2006). Influence of ion energy on properties of Mg alloy thin films formed by ion beam sputter deposition, Surface and Coatings Technology, Vol. 200 (No. 22–23), pp. 6527–6532.
12. Li P., Lei M.K., Zhu X.P., Han X.G., Liu C. & Xin J.P. (2010). Wear mechanism of AZ31 magnesium alloy irradiated by high-intensity pulsed ion beam, Surface and Coatings Technology, Vol.204 (No.14): pp. 2152–2158.
13. Stippich F., Vera E., Wolf G. K., Berg G., Friedrich Chr., Enhanced corrosion protection of magnesium oxide coatings on magnesium deposited by ion beam-assisted evaporation, Surface and Coatings Technology, Vol. 103 (1998), pp. 29–35.
14. Y.W. Song, D.Y. Shan, E.H. Han, High corrosion resistance of electroless composite plating coatings on AZ91D magnesium alloys, Electrochimica Acta. Vol. 53 (2008), pp. 2135–2143.
15. Zhang, S.C., Duan, H.Q., Cai, Q.Z., Wei, B.K., Lin, H.T., Chen, W.C., Effects of the main alloying elements on microstructure and properties of magnesium alloys, Zhuzao/Foundry 50 (6), (2001), pp. 310–315.
16. Sun Jin-quan, Yan Zi-feng, Cui Hong-zhi, He Qing-kun, Yang Hong-guang, Xiao Cheng-zhu, Wear resistance property of AM60 magnesium alloy modified by plasma surface treatment, Materials Science Forum Vol. 686 (2011) pp. 382–387.
17. Cui Hong-zhi, Sun Jin-quan, Xiao Cheng-zhu, Yang Hong-guang, Microstructure and corrosion resistance of AM60 magnesium alloy modified by plasma surface treatment, Materials Science Forum Vol. 686 (2011) pp. 230–234.
18. Yan C., Bai R.X., Gu Y.T., Ma W.J., Investigation on mechanical behaviour of AM60 magnesium alloys, Journal of Achievements in Materials and Manufacturing Engineering, vol. 31 (2008), issue 2, pp. 398–401.
19. Qi Qingju, Liu Yongbing, Yang Xiaohong, Friction and Wear Characteristics of Mg-AI Alloy Containing Rare Earths, Journal of Rare Earths, Vol. 21 (3003), No 2, pp. 157–162.
20. Tryliński W.: Drobne mechanizmy i przyrządy precyzyjne, WNT, Warszawa 1978.

Streszczenie

Stopy aluminium wykorzystywane w przemyśle samochodowym z powodu ich małej gęstości i dobrej wytrzymałości czasem współpracują z elementami stalowymi. Celem badań było zmierzenie oporów ruchu w styku stali po stopie magnezu AM60 (Mg6Al0.15Mn) oraz znalezienie sposobu na zmniejszenie tych oporów. Trudne warunki współpracy takich elementów mogą być poprawione poprzez cieplną obróbkę powierzchniową, na przykład powierzchniowe przetapianie plazmowe lub laserowe. Wartości współczynnika tarcia zmniejszają się niemal liniowo wraz ze wzrostem średniego nacisku powierzchniowego w styku. Uzyskane na pokazanym w artykule tribotesterze do tarcia wiertnego wartości współczynnika tarcia w styku stal ŁH15 po stopie AM60 (Mg6Al0.15Mn) mogą być 2.5 razy większe w porównaniu z odpowiednimi wartościami w styku stali ŁH15-C45 i mogą być dwa razy większe od wartości uzyskanych na tribotesterze trzpień po tarczy. To może być spowodowane większymi wartościami średniego nacisku powierzchniowego w strefie styku i średniej prędkości poślizgu w przypadku testera do tarcia wiertnego.